

Temperature- and Pressure-Induced Phase Transition in Tetrafluoro-1,4-benzoquinone Crystal

Akihiko Ikuta, Yoshio Suzuki,[†] Yoshinori Nibu, Hiroko Shimada,* and Ryoichi Shimada[†]

Department of Chemistry, Faculty of Science, Fukuoka University, Nanakuma, Jonan-ku, Fukuoka 814-0180

[†]Department of Electronics, Faculty of Technology, Fukuoka Institute of Technology, Wajiro-Higashi, Higashi-ku, Fukuoka 811-0295

(Received November 24, 1998)

The temperature and pressure effects on the Raman-active inter- and intramolecular vibrations of tetrafluoro-1,4-benzoquinone crystal were studied. The diffuse Raman bands observed in the intermolecular vibrational spectrum could be resolved with decreasing temperature or increasing pressure. The observed spectral structure due to the intermolecular vibrations changed as the temperature fell and also as the pressure increased. The vibrational frequencies of some intramolecular vibrational bands changed discontinuously under a certain pressure when the applied pressure was increased. The calculated pressure-induced frequency shifts for these vibrations deviate from the observed frequency shifts under high pressure. The DSC curve shows no distinct endothermic or exothermic peaks at temperatures between 77 and 520 K. These observations indicate that a displacive phase transition takes place at a temperature of around 180 K under 1 atm or under a pressure of 0.8 GPa at 300 K in a tetrafluoro-1,4-benzoquinone crystal.

The quinonoid structures of the 1,4-benzoquinone derivatives play important roles as electron acceptors in biological processes, and also for forming charge-transfer complexes. In order to investigate such interesting natures of the quinonoids by means of spectroscopic techniques, basic spectroscopic data are needed.

The crystal structures of 1,4-benzoquinone, tetrafluoro- and tetrachloro-1,4-benzoquinones have been studied by many workers.^{1–6} They showed that no phase transitions take place for 1,4-benzoquinone and tetrafluoro-1,4-benzoquinone crystals,^{1–3} while a displacive phase transition takes place for the tetrachloro-1,4-benzoquinone crystal.^{4–6} The Raman and infrared spectra of 1,4-benzoquinone,⁷ tetrafluoro-1,4-benzoquinone,⁸ and tetrachloro-1,4-benzoquinone crystals⁹ were observed in the inter- and intramolecular vibrational regions, and assignments for the inter- and intramolecular vibrations were made.

The Raman spectrum gives good information to study the phase transitions in molecular crystals, because intermolecular vibrations are generally observed in vibrational regions lower than 150 cm⁻¹, and bands having such low frequency can be easily observed in the Raman spectrum. Studies of phase transitions in molecular crystals through observing the Raman spectrum were made for benzene,^{10,11} dihalogenobenzenes,¹² tetrahalogenobenzenes,^{13,14} and pyrazine.¹⁵ A number of theoretical studies were also made for the pressure-induced frequency shift of the intramolecular vibrations by considering the intermolecular forces.^{16–19}

In this work, the phase transition of tetrafluoro-1,4-benzoquinone crystal is discussed based on observations of the temperature and pressure effects on the inter- and intramolecular

vibrations as well as on calculations of the pressure-induced frequency shifts of intramolecular vibrations.

Experimental

Material. Tetrafluoro-1,4-benzoquinone (fluoranyl), obtained from Aldrich Chemical Co., was used without further purification. The sample was powdered as finely as possible with a mortar and pestle.

Optical Measurement. The Raman spectra of fluoranyl crystal in the inter- and intramolecular vibrational regions were measured with a JEOL 400T Laser Raman Spectrophotometer and Bio-Rad FT-Raman II NBR-9001 Spectrophotometer. The spectra were observed at various temperatures between 300 and 77 K under 1 atm and under various pressures from 1 atm (1×10^{-4} GPa) to 3.6 GPa at 300 K by the backscattering observation method. The 514.5, 488.0, and 476.5 nm beams from an Ar⁺-ion laser of Spectra Physics Model 168B and a 1064 nm beam from a Nd:YAG laser of Spectra Physics Model T10-106C were used for excitation. A cryostat of OXFORD DN1704 was used for measuring the Raman spectra at low temperatures, and a diamond anvil cell obtained from Toshiba Tungaloy Co. was used to measure the Raman spectra under high pressures.

The method used to observe the Raman spectrum was exactly the same as previously described.^{13,14} A polarization measurement showed that the powder sample gave unpolarized Raman bands. The pressure inside the gasket hole was measured based on the wavelength shift of the R₁ fluorescence line at 694.2 nm emitted from ruby chips, using an equation proposed by Mao et al.²⁰ The pressure inside the hole was confirmed to be hydrostatic by observing the shapes of the R₁ and R₂ (692.7 nm) fluorescence lines emitted from the ruby.

A differential scanning calorimeter (DSC) curve was obtained with a Seiko denshi Model SSC/5200 at a heating rate of 5 °C min⁻¹

in the temperature range between 77 and 520 K under 1 atm.

Results and Discussion

Temperature Effect on Intermolecular Vibrations.

The low-frequency Raman spectra of a fluoranil crystal observed at various temperatures between 300 and 77 K are shown in Fig. 1 and the curves for the temperature dependence on the vibrational frequency (temperature–frequency curves) are given in Fig. 2. Figure 1 shows that the spectral structure changes as the temperature falls. The Raman spectrum observed at 300 K consists of two bands, a and d, where band a is not resolved well due to overlap with the strong Rayleigh-scattering line at temperatures of between 300 and 220 K. Band a shifts to the high-frequency side with decreasing temperature and splits into a doublet, bands a and b, below 120 K. A weak band c is observed below 270 K and the intensity of the band gradually increases with decreasing temperature. The intensity ratio of band c to band d becomes almost constant below 180 K. The spectrum observed at 77 K consists of four well-resolved bands (a, b, c, and d). The observed spectral changes in Fig. 1 suggest that the intermolecular interaction in fluoranil crystal changes as

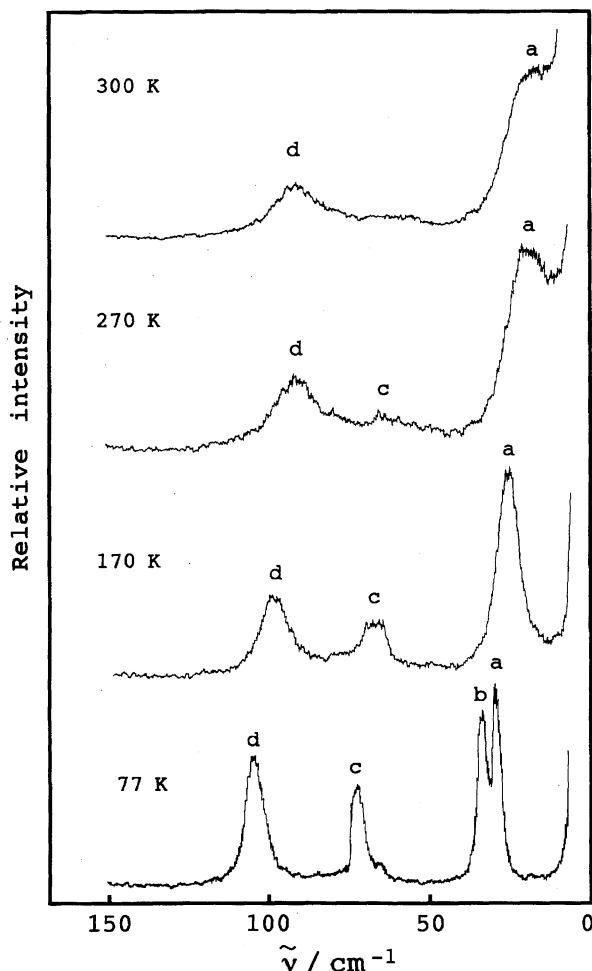


Fig. 1. The Raman spectra of fluoranil crystal in the intermolecular vibrational region observed at various temperatures between 300 and 77 K under 1 atm.

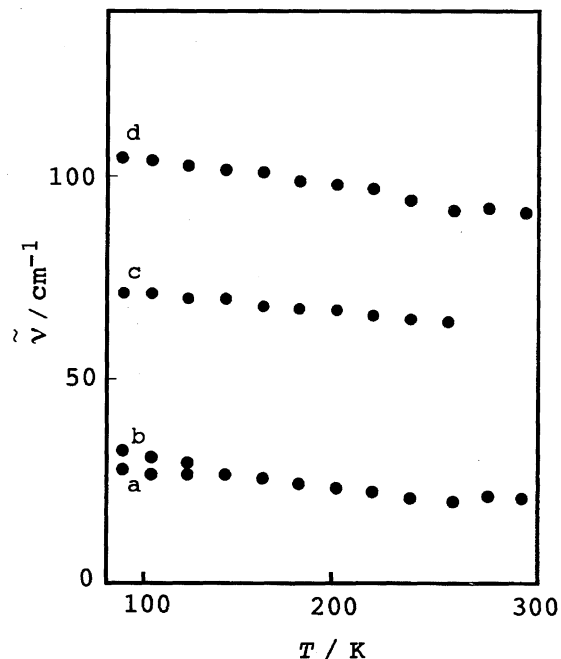


Fig. 2. Temperature–frequency curves for the Raman bands of fluoranil crystal in the intermolecular vibrational region observed at various temperatures between 77 and 300 K under 1 atm.

the temperature falls and the phase transition takes place at a temperature of around 180 K under 1 atm.

Figure 2 shows that the frequencies of bands a, b, c, and d increase continuously with decreasing temperature. The frequencies of the Raman bands observed at 300 and 77 K are given in Table 1 together with the frequencies of the bands observed under a pressure of 3.5 GPa at 300 K.

Pressure Effect on Intermolecular Vibrations. The Raman spectra of a fluoranil crystal observed under various pressures in the intermolecular vibrational region are given in Fig. 3, and curves for the pressure dependence on the vibrational frequency (pressure–frequency curves) are shown in Fig. 4. The Raman spectrum observed under 1 atm consists of two bands (a and d). The behavior of the change in the spectral structure caused by an increase in the applied pressure closely resembles to the behavior observed in the case of decreasing temperature.

The spectral structure gradually changes with increasing pressure. A shoulder band (b) is observed in the high-frequency side of band a under pressures above 1.2 GPa, and

Table 1. Raman Frequencies of the Intermolecular Vibrations of Fluoranil Crystal

Band	1 atm		300 K
	300 K $\tilde{\nu}/\text{cm}^{-1}$	77 K $\tilde{\nu}/\text{cm}^{-1}$	3.5 GPa $\tilde{\nu}/\text{cm}^{-1}$
a	16	29	43
b	16	32	57
c		72	112
d	89	103	143

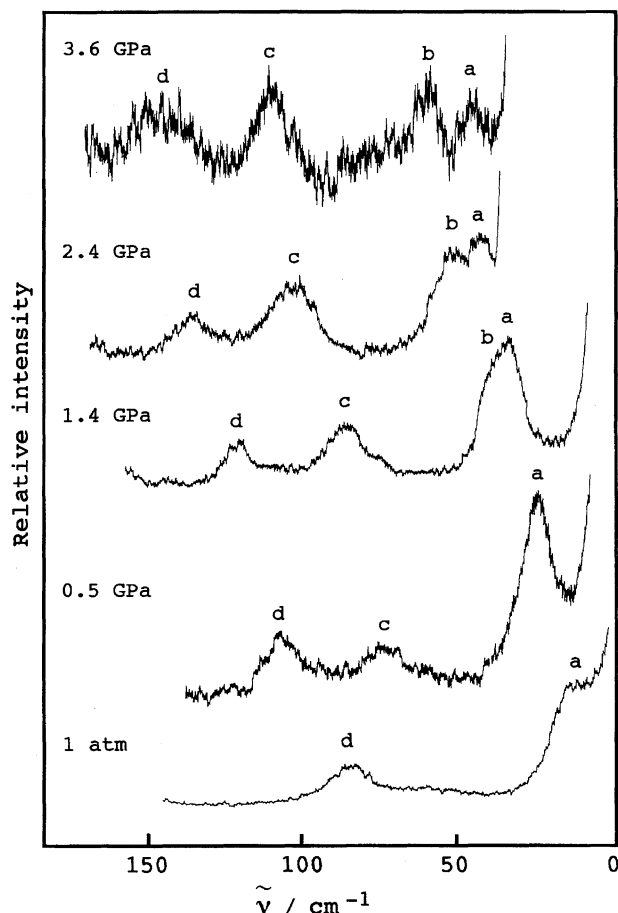


Fig. 3. The Raman spectra of fluoranil crystal in the intermolecular vibrational region observed under various pressures between 1 atm and 3.6 GPa at 300 K.

clearly separates from band a under pressures above 2 GPa. A very weak and diffuse band (c) is observed under pressures above 0.3 GPa, and the intensity of the band increases with increasing pressure. The ratio of the intensity of the band c to band d becomes almost constant under pressure above 0.8 GPa. The spectrum consists of four clearly resolved bands (a, b, c, and d) under pressures between 2 and 3.6 GPa. The spectral structure observed under pressures above 2 GPa corresponds well to the spectral structure observed at 77 K. These spectral changes in Fig. 2 suggest that the intermolecular interaction in fluoranil crystal changes with increasing pressure, and that the phase transition takes place under a pressure of 0.8 GPa at 300 K.

Pressure Effect on Intramolecular Vibrations. A normal-coordinate calculation was performed through the standard GF matrix method using a NEC UP4800/650 computer at computer center of Fukuoka University. The molecular structure of fluoranil was taken from the data determined by Meresse et al.¹⁾ The F-matrix elements for the in-plane and out-of-plane vibrations were evaluated with the potential of an improved modification of the Urey–Bradley and valence force fields, respectively, in the same way as described previously.^{21,22)} The values of the force constants for the in-plane and out-of-plane vibrations are given in Ta-

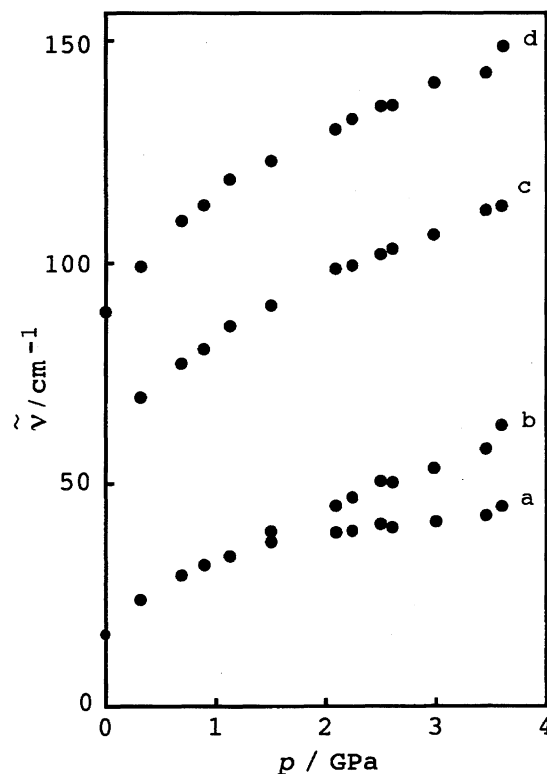


Fig. 4. Pressure–frequency curves for the Raman bands of fluoranil crystal in the intermolecular vibrational region observed under various pressures between 1 atm and 3.6 GPa at 300 K.

Table 2. Force Constants for the In-plane and Out-of-plane Vibrations of Fluoranil

In-plane		Out-of-plane	
$K_{C'=O}$	9.3	$Q_{C'-C}$	0.26
$K_{C'-C}$	2.8	$Q_{C=C}$	0.7
$K_{C=C}$	6.8	P_O	0.4
K_{C-F}	5.2	P_F	0.36
$H_{CC'C}$	0.55	$q_{C'-C,C=C}^0$	-0.03
$H_{OC'C}$	0.25	$q_{C'-C,C-C'}^0$	-0.07
$H_{C'CC}$	0.3	q^m	0.03
$H_{FCC'}$	0.1	$p_{O,F}^0$	0.01
H_{FCC}	0.14	$p_{F,F}^0$	0.02
$F_{C...C}$	0.4	$p_{O,F}^m$	-0.01
$F_{O...C}$	0.7	$p_{F,F}^m$	-0.02
$F_{C'...C}$	0.6	$p_{O,O}^0$	0.13
$F_{F...C'}$	0.8	$t_{O,C'-C}^0$	-0.1
$F_{F...C}$	1.2	$t_{F,C-C'}^0$	0.01
$k_{C=O,C=C}$	-0.4	$t_{F,C-C}^0$	0.03
$k_{C-F,C-F}^0$	0.8	$t_{O,C-C}^m$	-0.13
$k_{C'=O,C'=O}$	0.2	$t_{F,C-C'}^m$	0.05
$f_{\beta,\beta}^0$	-0.1		

Force constants denoted by K , H , F , and k are given in hN m^{-1} ($= \text{mdyn}/\text{\AA}$) and f , Q , P , q , p , and t in aN m rad^{-2} ($= \text{mdyn } \text{\AA}/\text{rad}^2$) units. C' is carbon atom bonded to O atom. β refers to bending of $\angle FCC$ angle.

ble 2. The notations of the force constants are the same as those described previously.^{21,22)} The calculated vibrational frequencies and modes are listed in Table 3.

Table 3. Normal Vibrations of Fluoranyl

Sym	Mode	This work		Girlando ^{a)}
		Obsd $\tilde{\nu}/\text{cm}^{-1}$	Calcd $\tilde{\nu}/\text{cm}^{-1}$	Obsd $\tilde{\nu}/\text{cm}^{-1}$
a_g	C=C + C=O str	1705	1717	1704
	C=C - C=O str	1680	1685	
	C-F str	1252	1232	1251
	ν_1	549	571	549
	ν_{6a}	427	440	425
	F bend	274	276	273
b_{3g}	C-C str	1376	1367	1374
	C-F str	1113	1097	1107
	F bend	781	802	
	ν_{6b}	427	413	(420)
	O bend	297	312	290
b_{1u}	C=O str	1701		1705
		1691	1693	1693
	C-F str	1335	1326	1334
		1327		1327
	C-C str	1046	1028	1046
	ν_{12}	632	611	632
b_{2u}	F bend	314	302	314
	C=C str	1677	1660	1677
	ν_{14}	1313	1291	1318
	C-F str	994	1004	995
				370
b_{1g}	O bend	370	352	367
	F bend	296	287	295
b_{2g}	F wag	360	346	358
	ν_4	781	781	780
a_u	F wag	488	482	488
				370
b_{3u}	O wag	159	164	158
	F wag		712	
a_u	ν_{16a}		161	
	O wag	737	725	
b_{3u}	F wag	217	237	224
				214
b_{3u}	ν_{16b}	117	123	116

a) A. Girlando and C. Pecile, *J. Chem. Soc., Faraday Trans. 2*, **71**, 689 (1975).

The Raman spectrum of a fluoranyl crystal in the intramolecular vibrational region observed under 1 atm at 300 K is shown in Fig. 5. The Raman bands observed at 1705, 549, 427, and 159 cm^{-1} were assigned to the C=C+C=O stretching vibration of a_g symmetry species, ν_1 (ring breathing vibration) of a_g species, ν_{6a} (ring deformation vibration) of a_g species, and O-wagging vibration of b_{2g} species, respectively.⁸⁾ The observed vibrational frequencies of the normal vibrations are listed in Table 3 together with the data given by Girlando.⁸⁾ The assignment given in this work is the same as that given by Girlando, except for the fact that the three bands due to C=C-C=O stretching vibrations of a_g species, F-bending vibration of b_{3g} species, and O-wagging vibration of b_{3u} species were newly detected in this work.

A discussion of the observed and calculated pressure-induced frequency shifts is made for the C=C+C=O stretching

(a_g), ν_1 , ν_{6a} , and O-wagging vibrations (b_{2g}). The spectrum was also observed under the pressures of between 1 atm and 3.6 GPa. The spectral structure observed under high pressures is essentially the same as that observed under 1 atm,⁸⁾ except that the bands shift to the high-frequency side with increasing pressure.

The curves of the plot of the observed frequency shift ($\Delta\tilde{\nu}$), defined by $\tilde{\nu}_p \text{ GPa} - \tilde{\nu}_1 \text{ atm}$, against the applied pressure (pressure-frequency shift curve) for these vibrations are shown in Fig. 6, where $\tilde{\nu}_p \text{ GPa}$ and $\tilde{\nu}_1 \text{ atm}$ are the vibrational frequencies observed under pressures of p GPa and 1 atm, respectively. The frequency shifts for the ν_{6a} and ν_1 vibrations increase monotonously with increasing pressure up to 3.6 GPa. The pressure-frequency shift curves for the C=C+C=O stretching and O-wagging vibrations show a discontinuous change of the slopes under a pressure of 0.8 GPa, and the frequency shifts increase again monotonously with increasing pressure up to 3.6 GPa. The ratio of the increment of the shift is 2–12 $\text{cm}^{-1} \text{ GPa}^{-1}$, depending on the vibrational modes.

The values of the pressure-induced frequency shifts were calculated for the C=C+C=O stretching, ν_1 , ν_{6a} , and O-wagging vibrations under various pressures from 1 atm to 3.5 GPa. The contribution of the neighboring sixteen molecules was taken into account concerning the frequency shift in the same manner as described previously.^{13,14)} The parameters for the intermolecular potential were taken from the data given by Spackman.²³⁾ The geometry and the orientation of the molecule in crystal were taken from the data given by Meresse et al.,¹⁾ and were assumed to remain unchanged upon the application of pressure. Since the value of the compressibility of fluoranyl crystal was not available, the value given for the hexachlorobenzene crystal²⁴⁾ was used. The displacement vectors of the atoms due to the normal vibrations of the fluoranyl molecule, which are necessary to calculate the pressure-induced frequency shifts, were obtained from the normal-coordinate calculation described above. The observed and calculated pressure-induced frequency shifts are shown in Fig. 6 by full and open circles, respectively. The values of the calculated frequency shifts under a pressure of 3.5 GPa are given in Table 4, together with the observed values. The calculation indicates that the repulsive intermolecular forces give the main contribution to the pressure-induced frequency shifts of the intramolecular vibrations rather than the dispersion and electrostatic intermolecular forces, as in the cases of the general molecular crystals.^{13–15)}

The agreement between the calculated and observed frequency shifts is quite good for the ring vibrations of the ν_1 and ν_{6a} modes. The observed frequencies for these vibrations shift continuously to the high-frequency side with increasing pressure. On the other hand, the calculated frequency shifts deviate from the observed frequency shifts for the C=C+C=O stretching and O-wagging vibrations. The observed pressure-frequency shift curves for these vibrations show a discontinuous change of the slopes under a pressure of 0.8 GPa. These observations suggest that the intermolecular interaction changes under a pressure of 0.8 GPa, and

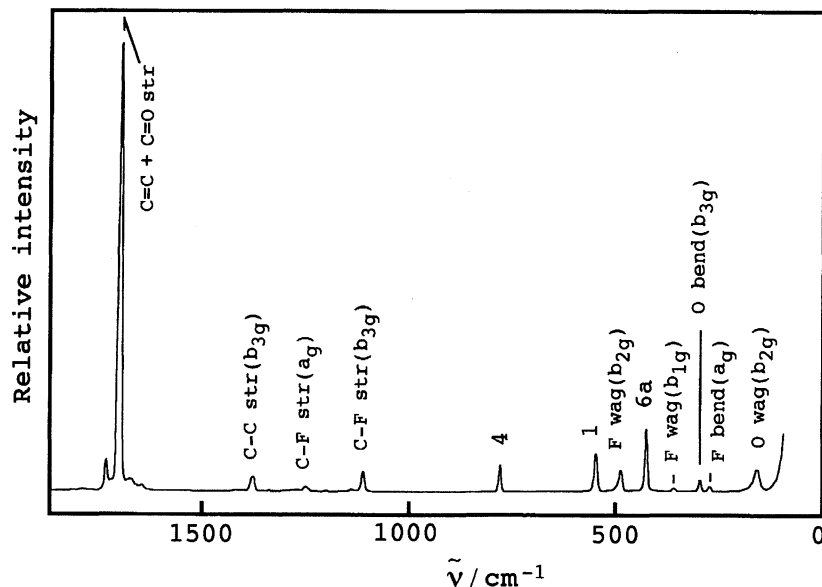


Fig. 5. The Raman spectrum of fluoranil crystal in the intramolecular vibrational region observed under 1 atm at 300 K.

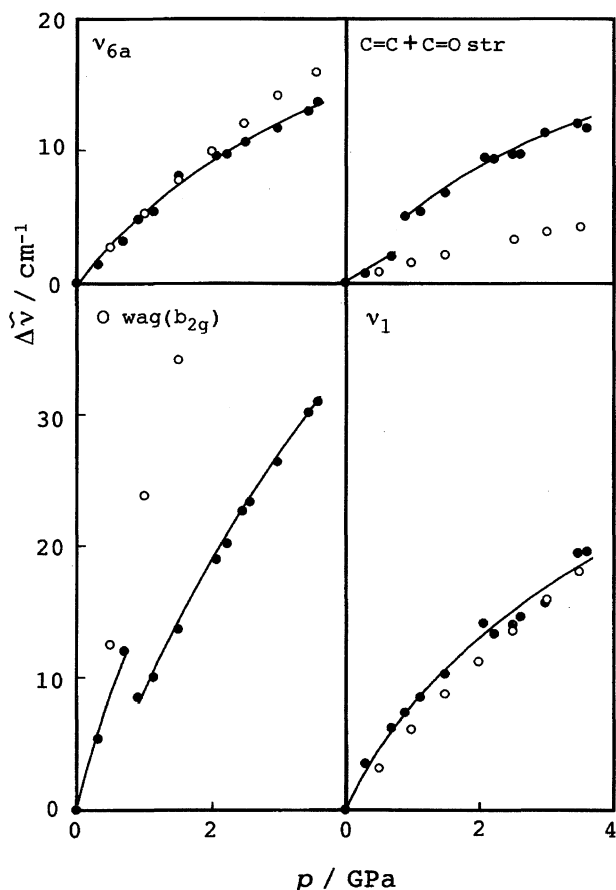


Fig. 6. Pressure-frequency shift curves for the intramolecular ν_{6a} , O-wagging, C=C+C=O stretching, and ν_1 vibrations of fluoranil. The frequency shift $\Delta\tilde{\nu}$ is defined by $(\tilde{\nu}_p \text{ GPa} - \tilde{\nu}_1 \text{ atm})$. The marks ● and ○ refer to the observed and calculated frequency shifts, respectively.

that a change in the interaction causes a deviation of the calculated pressure-induced frequency shift from the observed shift under a pressure above 0.8 GPa. It is considered that a

Table 4. Calculated and Observed Pressure-Induced Frequency Shifts for Some Intramolecular Vibrations of Fluoranil Crystal under 3.5 GPa

Mode	$\tilde{\nu}_{3.5\text{GPa}} - \tilde{\nu}_{1\text{ atm}}$				
	Calcd				Obsd
	Repul	Disp	E.S.	Total	
	$\tilde{\nu}/\text{cm}^{-1}$	$\tilde{\nu}/\text{cm}^{-1}$	$\tilde{\nu}/\text{cm}^{-1}$	$\tilde{\nu}/\text{cm}^{-1}$	$\tilde{\nu}/\text{cm}^{-1}$
C=C + C=O str	4.98	-0.85	0.0	4.13	13
ν_1	20.98	-2.95	0.0	18.03	20
ν_{6a}	19.04	-2.82	0.0	16.22	14
O wag (b_{2g})	79.10	-11.09	0.0	68.01	32

change in the intermolecular interaction gives rise to a phase transition, just as observed for the 1,2,4,5-tetrachlorobenzene crystal.¹³⁾ The phase transition has a slight effect on the pressure-induced frequency shifts for the ν_1 and ν_{6a} vibrations, while the transition has a remarkable effect on the frequency shifts for the C=C+C=O stretching and O-wagging vibrations. The behavior of the frequency shifts can be reasonably explained by the displacements of the side bonds involving in these vibrational modes.

Cansell et al.²⁵⁾ studied the phase transition of the benzene crystal, and showed that the phase transition could not be detected unambiguously through a survey of the pressure-frequency curve for the intramolecular vibrations. They also showed that the plot of the bandwidth against the applied pressure at constant temperature (pressure-bandwidth curve) showed a distinct change in the slope of the curve due to the phase transition. Maehara et al. also showed that a clear detection of the phase transition in the pyrazine crystal could be made by a survey of the pressure-bandwidth curve.¹⁵⁾

The temperature-bandwidth curves for the O-wagging, ν_1 , and C=C+C=O stretching vibrations observed under 1 atm and the pressure-bandwidth curves observed at 300 K are

given in Figs. 7 and 8, respectively. Discontinuous changes in the slope were clearly found in temperature–bandwidth curves observed at a temperature of 180 K and in pressure–bandwidth curves observed under a pressure of 0.8 GPa for the O–wagging and C=C+C=O stretching vibrations. On the other hand, no discontinuous changes in the slope were clearly found in the temperature–bandwidth and pressure–bandwidth curves for the ν_1 vibration. For this vibration, no discontinuous change in the slope could be detected in the pressure–frequency curve.

The curve obtained by a differential-scanning calorimetric measurement (DSC curve) for the fluoranyl crystal (Fig. 9) shows no distinct endothermic or exothermic peaks at temperatures of between 77 and 520 K, except for a sharp endothermic peak at 456 K due to the melting point of the fluoranyl crystal.

The observed facts for temperature and pressure effects on the inter- and intramolecular vibrations and for DSC curve lead to the conclusion that a phase transition takes place in the fluoranyl crystal at a temperature of around 180 K under 1 atm, or under a pressure of 0.8 GPa at 300 K. The phase transition may not accompany a change in the space group of the crystal, but may be a displacive transition.

The authors thank the Japan Private School Promotion Foundation for Science Research Promotion Fund.

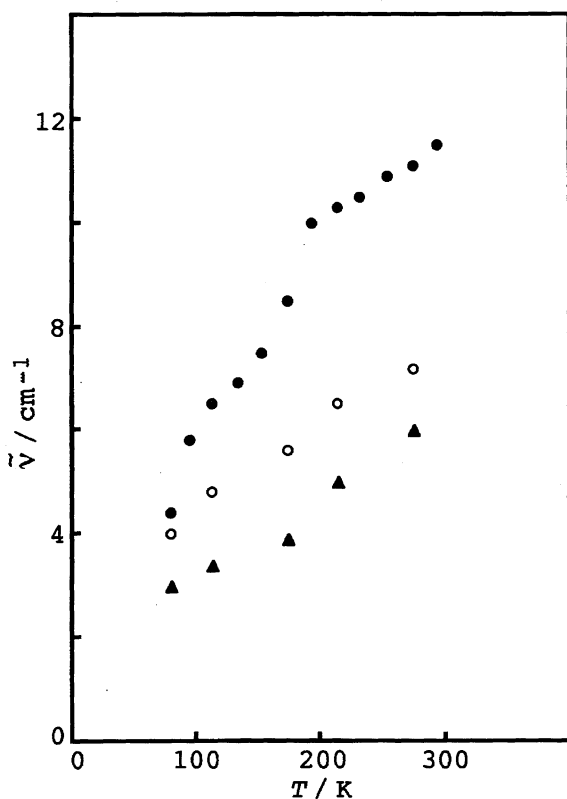


Fig. 7. Temperature–bandwidth curves for the C=C+C=O stretching, ν_1 , and O–wagging vibrations of fluoranyl observed under 1 atm. The marks \blacktriangle , \circ , and \bullet refer to the bandwidth of the C=C+C=O stretching, ν_1 , and O–wagging vibrational bands, respectively.

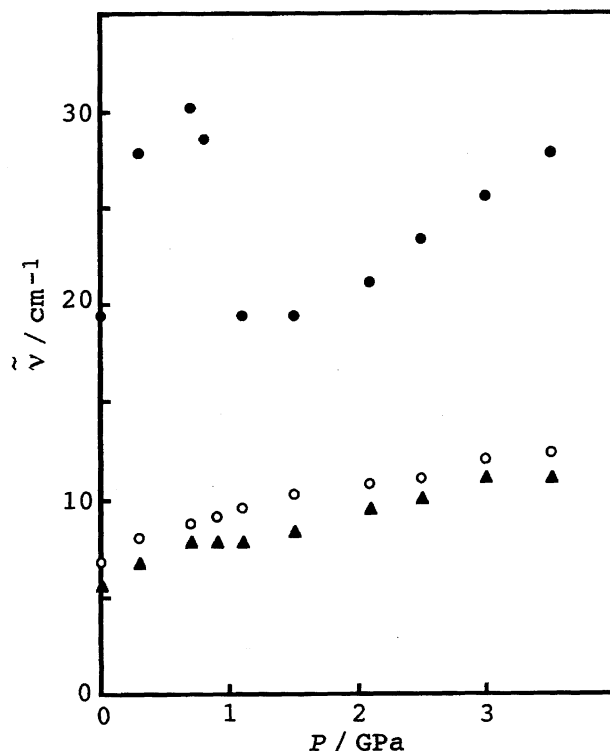


Fig. 8. Pressure–bandwidth curves for the C=C+C=O stretching, ν_1 , and O–wagging vibrations of fluoranyl observed at 300 K. The marks \blacktriangle , \circ , and \bullet refer to the bandwidths of the vibrational bands in the manner way as Fig. 7.

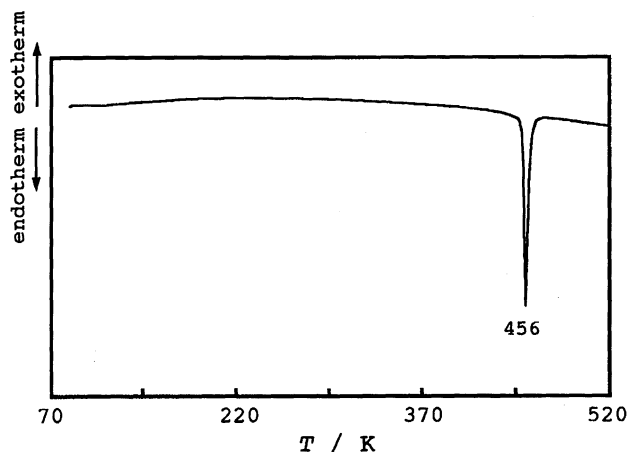


Fig. 9. DSC curve of fluoranyl crystal measured at the temperatures between 77 and 520 K.

References

- 1) P. A. Meresse, C. Courseille, and N. B. Chanh, *Acta Crystallogr., Sect. B*, **B30**, 524 (1974).
- 2) K. Hagen and D. G. Nicholson, *Acta Crystallogr., Sect. B*, **B43**, 1959 (1987).
- 3) J. Wang and D. F. R. Gilson, *Spectrochim. Acta, Part A*, **52A**, 755 (1996).
- 4) S. S. C. Chu, G. A. Jeffrey, and T. Sakurai, *Acta Crystallogr.*, **15**, 661 (1962).

- 5) A. Girard, Y. Delugeard, C. Ecolivet, and H. Cailleau, *J. Phys. C: Solid State Phys.*, **15**, 2127 (1982).
 - 6) Y. Kubozono, T. Yoshida, H. Maeda, S. Kashino, H. Terauchi, and T. Ishii, *J. Phys. Chem. Solids*, **58**, 1375 (1997).
 - 7) B. Lunelli and C. Pecile, *Spectrochim. Acta, Part A*, **29A**, 1989 (1973).
 - 8) A. Girlando and C. Pecile, *J. Chem. Soc., Faraday Trans. 2*, **71**, 689 (1975).
 - 9) A. Girlando and C. Pecile, *J. Chem. Soc., Faraday Trans. 2*, **69**, 1291 (1973).
 - 10) W. D. Ellenson and M. Nicol, *J. Chem. Phys.*, **61**, 1380 (1974).
 - 11) M. M. Thiery and J. M. Leger, *J. Chem. Phys.*, **89**, 4255 (1988).
 - 12) D. M. Adams and I. O. C. Ekejiuba, *J. Chem. Soc., Faraday Trans.*, **77**, 851 (1981).
 - 13) S. Matsukuma, H. Kawano, Y. Nibu, H. Shimada, and R. Shimada, *Bull. Chem. Soc. Jpn.*, **67**, 1588 (1994).
 - 14) F. Shimizu, K. Yoshikai, H. Kawano, Y. Nibu, H. Shimada, and R. Shimada, *Bull. Chem. Soc. Jpn.*, **69**, 947 (1996).
 - 15) M. Maehara, H. Kawano, Y. Nibu, H. Shimada, and R. Shimada, *Bull. Chem. Soc. Jpn.*, **68**, 506 (1995).
 - 16) R. M. Hexer, *J. Chem. Phys.*, **33**, 1833 (1960).
 - 17) D. A. Dows, *J. Chem. Phys.*, **32**, 1342 (1960).
 - 18) F. D. Verderame, J. A. Lannon, L. E. Harris, W. G. Thomas, and E. A. Lucia, *J. Chem. Phys.*, **56**, 2638 (1972).
 - 19) P. J. Miller, S. Block, and G. J. Piermarini, *J. Phys. Chem.*, **93**, 462 (1989).
 - 20) H. K. Mao, P. M. Bell, J. W. Shaner, and D. J. Steinberg, *J. Appl. Phys.*, **49**, 3276 (1978).
 - 21) S. Kizuki, Y. Ishibashi, H. Shimada, and R. Shimada, *Mem. Fac. Sci. Kyushu Univ. Ser. C*, **13**, 7 (1981).
 - 22) S. Nakama, H. Shimada, and R. Shimada, *Bull. Chem. Soc. Jpn.*, **57**, 2584 (1984).
 - 23) M. A. Spackman, *J. Chem. Phys.*, **85**, 6579 (1986).
 - 24) S. N. Vaidya and G. C. Kennedy, *J. Chem. Phys.*, **55**, 987 (1971).
 - 25) F. Cansell, D. Fabre, and J. P. Petit, *J. Chem. Phys.*, **99**, 7300 (1993).
-